

# Multipole Analysis of Radio-Frequency Reactions in Ultra-Cold Atoms

Betzalel Bazak, Evgeny Liverts and Nir Barnea

*The Racah Institute of Physics, The Hebrew University, 91904, Jerusalem, Israel*

(Dated: June 28, 2018)

Using the multipole expansion we analyze photo induced reactions in an ultra-cold atomic gas composed of identical neutral bosons. While the Frank-Condon factor dominates the photo induced spin-flip reactions, we have found that for frozen-spin process where the atomic spins are conserved the reaction rate is governed by the monopole  $r^2$  and the quadrupole terms. Consequently, the dependence of the frozen-spin reaction rate on the photon wave number  $k$  acquires an extra  $k^4$  factor in comparison to the spin-flip process. Comparing the relative strength of the  $r^2$  and quadrupole modes in dimer photoassociation we predict that the mutual importance of these two modes changes with temperature and scattering length.

PACS numbers: 25.10.+s, 25.20.-x, 67.85.-d, 31.15.ac

Radio-Frequency (rf) association of molecules in ultra-cold atomic traps is an invaluable experimental tool for studying the universal properties of few-body systems [1, 2]. In such experiments [3–10] rf induced dimer or trimer formation leads to enhanced atom loss rate due to larger probability for three-body recombination. The measured atom loss rate as a function of the rf field frequency incorporates the data about the various molecular thresholds and structures, and can be used to calibrate the two-body scattering length and to measure the three-body binding energy.

Photo-integration of molecules, where resonant rf radiation is used to stimulate photon emission, is closely related, through time reversal, to electro-weak reactions in light nuclei. In fact, rf photoreactions inducing an atomic spin-flip are governed by the Frank-Condon factor. This factor is the atomic analog of the Fermi operator, which at low momentum transfer describes the charged vector-current neutrino induced isospin-flip reactions in nuclear systems. The nuclear analog to frozen-spin rf reactions is photoabsorption, where an incoming photon dissociates the nucleus. For example, photoreactions within the  $\alpha$ -cluster model of nuclei such as  $^{12}\text{C}$ ,  $^{16}\text{O}$  are governed by the same physical mechanisms studied here. Therefore, studying rf photoreactions in ultra-cold atomic systems can be instrumental for understanding the nuclear dynamics, the complicated nuclear continuum, and for predicting unmeasurable electro-weak cross-sections of astrophysical importance.

Previous analysis of these rf experiments [11–14], have relied on the Franck-Condon factor estimating the transition rates. While this approach is appropriate for describing spin-flip reactions, it is not suitable for frozen-spin reactions. In [15] we have studied the quadrupole contribution to the frozen-spin response of a bound bosonic trimer. In this article we present a complete multipole analysis of the rf association process forming a bound molecule composed of  $N$  identical bosons. We show that the spin-flip and frozen-spin processes differ by their operator structure and by the de-excitation modes that contribute to the photoassociation rate. We apply our results to study frozen-spin dimer formation. We focus on

bosonic alkali-metal atoms, in which a single  $s$ -shell valence electron is coupled to an half-integer spin nucleus to form a boson. This is the case for  $^7\text{Li}$ ,  $^{23}\text{Na}$ ,  $^{39}\text{K}$ ,  $^{41}\text{K}$ ,  $^{85}\text{Rb}$ ,  $^{87}\text{Rb}$ , and  $^{133}\text{Cs}$ . Extension of our results to other atoms and fermionic isotopes is rather simple but lays outside the confines of the current manuscript.

In ultra-cold atomic traps, the trapped particles are subject to an external magnetic field  $\mathbf{B} = B\hat{z}$  applied to control the inter-atomic interaction, i.e. the scattering length, through a Feshbach resonance. Consequently, the energy of the system is dominated by the interactions of the valence electron spin  $S = 1/2$  with the external and the nuclear magnetic fields. The Zeeman interaction with the external magnetic field reads  $-g\mu_B\mathbf{S}\cdot\mathbf{B}$ , where  $g$  is the electron g-factor, and  $\mu_B$  is the Bohr magneton [16]. The hyperfine spin-nucleus contact interaction  $\hbar\omega_{hf}\mathbf{I}\cdot\mathbf{S}$  couples the electron with the nuclear spin  $\mathbf{I}$  where  $\omega_{hf}$  is the hyperfine splitting frequency. When both interactions are comparable, the total spin  $\mathbf{F} = \mathbf{I} + \mathbf{S}$  is not a good quantum number, however its projection  $m_F$ , is.

To be specific, we consider  $I = 3/2$ , the case for  $^7\text{Li}$ ,  $^{23}\text{Na}$ ,  $^{39}\text{K}$ ,  $^{41}\text{K}$ , and  $^{87}\text{Rb}$ . The atomic spin state composition in the  $|m_S, m_I\rangle$  basis,

$$|m_F\rangle = \sin\theta_{m_F}|1/2, m_F - 1/2\rangle + \cos\theta_{m_F}|-1/2, m_F + 1/2\rangle$$

is given by

$$\tan\theta_{m_F} = \begin{cases} \infty & m_F = 2 \\ (1 - 2\eta - 2\sqrt{1 - \eta + \eta^2})/\sqrt{3} & m_F = 1 \\ -\eta - \sqrt{1 + \eta^2} & m_F = 0 \\ -(1 + 2\eta + 2\sqrt{1 + \eta + \eta^2})/\sqrt{3} & m_F = -1 \end{cases} \quad (1)$$

for the low energy branch states. Here  $\eta = g\mu_B B/2\hbar\omega_{hf}$  is the ratio between the Zeeman and the hyper-fine splitting.

In photoassociation experiments, an rf radiation of few MHz is applied to the ultra-cold atomic gas. When the photon energy matches, stimulated emission occurs and a molecule is formed. Fermi's golden rule dictates the

transition rate of such process to be,

$$r_{i \rightarrow f} = \frac{2\pi}{\hbar} \sum_i \sum_f |\langle f, \mathbf{k}\rho | \hat{H}_I | i \rangle|^2 \delta(E_i - E_f - \hbar\omega_k), \quad (2)$$

where  $\sum_i$  averages on the appropriate initial states and  $\sum_f$  sums on the final states. Specifically,  $|i\rangle$  is the continuum state,  $\mathbf{k}\rho$  is the emitted photon momentum and polarization, and  $|f\rangle$  is the formed  $N$ -body bound state.

The interaction Hamiltonian  $\hat{H}_I = -\frac{e}{c} \int d\mathbf{x} \mathbf{J}(\mathbf{x}) \cdot \mathbf{A}(\mathbf{x})$  between an atomic system and an electromagnetic (EM) radiation field  $\mathbf{A}$  is defined by the current operator  $\mathbf{J}$  composed of convection and magnetization terms,  $\mathbf{J}(\mathbf{x}) = \mathbf{J}_c(\mathbf{x}) + c\nabla \times \boldsymbol{\mu}(\mathbf{x})$ . For a system of neutral atoms interacting with long wavelength radiation  $\mathbf{J}_c \approx 0$ , and the interaction between the radiation field and the system occurs through the magnetization density  $e\boldsymbol{\mu}(\mathbf{x}) = g\mu_B \sum_i \mathbf{S}_i \delta(\mathbf{x} - \mathbf{r}_i)$ . Using box normalization of volume  $\Omega$ , the EM field reads  $\mathbf{A}(\mathbf{x}) = \sum_{\mathbf{k}, \rho} \sqrt{\frac{\hbar c^2}{2\Omega\omega_k}} \hat{\mathbf{e}}_{\mathbf{k}\rho} (a_{\mathbf{k}\rho}^\dagger e^{i\mathbf{k}\cdot\mathbf{x}} + h.c.)$  where  $\rho = 1, 2$  are the photon linear polarizations,  $\omega_k$  is its frequency and  $\mathbf{k}$  is its momentum.

For an atomic system we can assume that the initial and final matter wave functions can be written as a product of spin and configuration space terms,  $\Psi = \Phi_{LM_L} \chi_{M_F}$ , where  $\Phi_{LM_L} = \Phi_{LM_L}(\mathbf{r}_1, \mathbf{r}_2, \dots, \mathbf{r}_A)$  is a symmetric  $N$ -particle wave function with angular momentum quantum numbers  $LM_L$  and  $\chi_{M_F} = \mathcal{S}[|m_F(1)\rangle |m_F(2)\rangle \dots |m_F(A)\rangle]$  is the symmetrized spin wave function with magnetic quantum number  $M_F = \sum_j m_F(j)$ . Using this factorization, The transition matrix element in (2) takes the form

$$\langle f, \mathbf{k}\rho | \hat{H}_I | i \rangle = -ig\mu_B \sqrt{\frac{\hbar c^2}{2\Omega\omega_k}} \sum_{j=1}^N \langle \chi_{M'_F}^f | \mathbf{S}_j \cdot (\mathbf{k} \times \hat{\mathbf{e}}_{\mathbf{k}\rho}) | \chi_{M_F}^i \rangle \langle \Phi_{L'M'_L}^f | e^{i\mathbf{k}\cdot\mathbf{r}_j} | \Phi_{LM_L}^i \rangle. \quad (3)$$

The spin operator can be written in spherical notation,  $\mathbf{S} \cdot (\mathbf{k} \times \hat{\mathbf{e}}_{\mathbf{k}\rho}) = \sum_\lambda (-)^{\lambda} S_{-\lambda} \cdot (\mathbf{k} \times \hat{\mathbf{e}}_{\mathbf{k}\rho})_\lambda$  where  $\lambda = 0, \pm 1$ . To calculate this quantity the laboratory  $\hat{z}$  axis is defined by the static magnetic field. The rotation from the laboratory reference frame  $(\hat{x}, \hat{y}, \hat{z})$ , to the photon reference frame,  $(\hat{e}, \hat{k} \times \hat{e}, \hat{k})$  is represented by Euler angles  $(\alpha, \beta, \gamma)$ . Then,  $(\hat{k} \times \hat{e}) \cdot \hat{z} = -\sin\gamma \sin\beta$ , and  $|(\hat{k} \times \hat{e})_{\pm 1}|^2 = (1 - \sin^2\gamma \sin^2\beta)/2$ .

For rf radiation the photon wavelength is much larger than the typical dimension of the system  $R$ , therefore  $kR \ll 1$  and the lowest order in  $kR$  dominates the interaction. The first contribution depends on the photon energy versus the energy difference between adjacent Zeeman states.

Using Eq. (1), the spin matrix elements can be easily

calculated to give,

$$\langle m'_F | S_\lambda | m_F \rangle = \delta_{m_F + \lambda, m'_F} \begin{cases} \sin\theta_{m'_F} \cos\theta_{m_F} & \lambda = +1 \\ -\frac{1}{2} \cos 2\theta_{m_F} & \lambda = 0 \\ \sin\theta_{m_F} \cos\theta_{m'_F} & \lambda = -1 \end{cases} \quad (4)$$

If the photon can induce a Zeeman state change, i.e. spin-flip, the leading contribution comes at order  $k$ . Energy is delivered to the system through the spin matrix element and we can approximate  $e^{i\mathbf{x}} \simeq 1$ , to get

$$|\langle f, \mathbf{k}\rho | \hat{H}_I | i \rangle|^2 = \frac{g^2 \mu_B^2 \hbar c k (1 - \sin^2\gamma \sin^2\beta) N^2}{4\Omega} \sum_{\lambda=\pm 1} |\langle \chi_{M'_F}^f | S_{j,\lambda} | \chi_{M_F}^i \rangle|^2 |\langle \Phi_{L'M'_L}^f | \Phi_{LM_L}^i \rangle|^2 \delta_{L,L'} \delta_{M_L, M'_L}. \quad (5)$$

The factor  $N^2$  results from utilizing the symmetry of the wave function and  $S_{j,\lambda}$  is the magnetic moment operator of any specific particle  $j$ . The last term on the rhs of Eq. (5) is just the Frank-Condon factor.

In frozen spin reactions  $\lambda = 0$  and the rf photon does not affect the spin structure of the system. Therefore  $M'_F = M_F$ ,  $|\chi_{M'_F}^f\rangle = |\chi_{M_F}^i\rangle$  and the transition matrix element can be written as

$$\langle f, \mathbf{k}\rho | \hat{H}_I | i \rangle = -ig\mu_B \sqrt{\frac{\hbar c^2}{2\Omega\omega_k}} k \sin\gamma \sin\beta \langle S_0 \rangle \langle \Phi_{L'M'_L}^f | \sum_{j=1}^N e^{i\mathbf{k}\cdot\mathbf{r}_j} | \Phi_{LM_L}^i \rangle, \quad (6)$$

where  $\langle S_0 \rangle = \langle \chi_{M'_F}^i | S_{1,0} | \chi_{M_F}^i \rangle$  is the average single particle magnetic moment.

In the long wavelength limit, the leading contributions to the photoreaction process are

$$\sum_{j=1}^N e^{i\mathbf{k}\cdot\mathbf{r}_j} \approx N + i \sum_{j=1}^N \mathbf{k} \cdot \mathbf{r}_j - \sum_{j=1}^N \frac{k^2 r_j^2}{6} - \sum_{j=1}^N 4\pi \frac{k^2 r_j^2}{15} \sum_m Y_{2-m}(\hat{k}) Y_{2m}(\hat{r}_j), \quad (7)$$

where  $Y_{lm}$  are the spherical harmonics. The difference between the four operators in (7) is clear. The first operator is proportional to 1 and stands for elastic interaction. For photon emission this kind of interaction defies energy conservation. The second term is just the dipole operator, which for identical particles is proportional to the center of mass and hence does not affect relative motion of the atoms. Therefore the only contributions to such excitation arises from the  $r^2$ , and the quadrupole terms. Consequently the transition probability scales as  $k^5$ . Summing over the initial and final magnetic numbers

$M_L, M'_L$ , the transition matrix element reads

$$\sum_{M_L} \sum_{M'_L} |\langle f, \mathbf{k}\rho | \hat{H}_I | i \rangle|^2 = \frac{4\pi\hbar c k^5 g^2 \mu_B^2 \sin^2 \gamma \sin^2 \beta N^2}{2\Omega} |\langle S_0 \rangle|^2 \left( \frac{1}{6^2} |\langle \Phi_{L'}^f \| r_j^2 Y_0 \| \Phi_{L'}^i \rangle|^2 + \frac{1}{15^2} |\langle \Phi_{L'}^f \| r_j^2 Y_2(\hat{r}_j) \| \Phi_{L'}^i \rangle|^2 \right). \quad (8)$$

Here, like in (5), we have used the symmetry of the wave function and  $\mathbf{r}_j$  is the coordinate of any of the particles  $j = 1, \dots, N$ . Comparing equations (8) and (5) the difference between spin-flip and frozen-spin reactions is evident. To begin with, the frozen-spin acquires an extra  $k^4$  factor suppressing the reaction rate. Then, we see that whereas the leading configuration space spin-flip operator is proportional to the unit operator, like the Fermi operator in nuclear physics, for frozen-spin reactions we identify two competing modes of order  $k^2$ , one is the  $r^2$  operator and the other is just the quadrupole operator.

Once established the operator structure of the transition rate we would like to focus our attention on frozen-spin photoassociation reactions trying to estimate the relative importance of the two reaction modes. To this end we consider the case of dimer formation, which under certain simplifying assumptions can be calculated analytically.

In the universal regime, where the scattering length is much larger than the potential range, one can approximate the wave functions by their asymptotic behavior. The dimer bound state with binding energy  $E_B$  is an  $s$ -wave state, and  $\Phi_{00}^f(\mathbf{r}) = Y_{00} \varphi_B(r)/r$  where  $\mathbf{r} = \mathbf{r}_2 - \mathbf{r}_1$  is the relative coordinate.  $\varphi_B(r) \cong \sqrt{2\kappa} e^{-\kappa r}$  and  $\kappa = \sqrt{m|E_B|/\hbar^2}$ . For the initial (continuum) states, the asymptotic scattering solution is used, i.e.  $\Phi_{LM}^f(\mathbf{r}) = Y_{LM} \phi_L(r)/r$ , where  $\phi_L(r) = \sqrt{2/Rqr} [j_L(qr) \cos \delta_L - y_L(qr) \sin \delta_L]$ ,  $\delta_L$  is the phase shift,  $j_L$  and  $y_L$  are the spherical Bessel functions of the first and second kind,  $q$  is the relative momentum, and the wave function is normalized in a sphere of radius  $R$ .

Given the  $L' = 0$  dimer ground state, the  $r^2$  term corresponds to  $L = 0$   $s$ -wave formation, while the quadrupole term to  $L = 2$   $d$ -wave formation. Using  $|\langle 0 \| Y_0 \| 0 \rangle|^2 = 1/4\pi$  and  $|\langle 2 \| Y_2 \| 0 \rangle|^2 = 5/4\pi$ ,

$$\begin{aligned} |\langle \Phi_0^f \| r^2 Y_0 \| \Phi_0^i \rangle|^2 &= \frac{1}{4\pi} I_s^2 \\ |\langle \Phi_0^f \| r^2 Y_2 \| \Phi_2^i \rangle|^2 &= \frac{5}{4\pi} I_d^2. \end{aligned} \quad (9)$$

Here  $I_s = \int_0^\infty \varphi_B^*(r) \phi_0(r) r^2 dr$ , and same for  $I_d$  replacing  $\phi_0$  by  $\phi_2$ . The transformation to the relative coordinate  $r$  in (9) adds an extra factor of  $1/16$  in (8).

For the  $s$ -wave mode, the radial integration yields

$$I_s = \frac{4q}{(q^2 + \kappa^2)^3} \sqrt{\frac{\kappa}{R}} \left[ (3\kappa^2 - q^2) \cos \delta_0 - \frac{\kappa}{q} (3q^2 - \kappa^2) \sin \delta_0 \right]. \quad (10)$$

At low scattering energy, the  $s$ -wave phase shift takes the form  $q \cot \delta_0 \cong -1/a_s + r_{eff} q^2/2$  where  $a_s$  is the scattering length and  $r_{eff}$  is the effective range. The dimer's binding energy is connected to these parameters by the relation [18]  $\kappa = 1/a_s + r_{eff} \kappa^2/2$ .

For the  $d$ -wave mode, the radial integration yields,

$$I_d = \frac{2q}{(q^2 + \kappa^2)^3} \sqrt{\frac{\kappa}{R}} \left[ 8q^2 \cos \delta_2 + \frac{\kappa}{q^3} (15q^4 + 10q^2 \kappa^2 + 3\kappa^4) \sin \delta_2 \right]. \quad (11)$$

For short-range potentials,  $\delta_L \approx q^{2L+1}$  as  $q \rightarrow 0$ , thus  $\delta_2 \approx (a_d q)^5$  where  $a_d$  is the  $d$ -wave ‘‘scattering length’’. We note that for the Van der Waals potential the correct threshold behavior is,  $\delta_2 \approx \pm (a_d q)^4$  [17]. As long as  $a_d$  is of the order of the effective range it is safe to assume  $\delta_2 \approx 0$ .

The relative contribution of the  $s, d$  modes to the dimer formation is displayed in Fig. 1, where the last term in parenthesis on the rhs of Eq. (8) is presented normalized, along with the  $s$  and  $d$  components. From the figure it can be seen that the  $s$ -wave association is peaked around  $q = \kappa/2$ , while the  $d$ -wave association is peaked at  $q = \kappa$ . For small  $a_s/r_{eff}$  ratio the  $d$ -wave is the dominant mode but as we approach the unitary limit  $a_s/r_{eff} \rightarrow \infty$  the  $s$ -wave becomes dominant. We note however, that as the  $a_s/r_{eff}$  ratio become smaller finite range corrections, ignored here, become more important. In photoassociation experiments angular analysis is impossible and therefore the different energy dependence of the two dimer formation modes, Fig. 1, can be used to distinguish between them. As it stands, the large overlap between the two modes will certainly complicate such an attempt.

The average of the initial states  $\bar{\sum}_i$  and the sum over the final states  $\sum_f$  are the last components needed for evaluating the dimer association rate, Eq. (2). The initial two-body state  $|i\rangle = |qLM_L\rangle$  describes two atoms in the continuum with relative momentum  $q$  and angular momentum  $L, M_L$ . The average on these states takes the form

$$\bar{\sum}_i = \sum_{L=0}^{\infty} \sum_{M_L=-L}^L \int_0^\infty dq P(qLM_L), \quad (12)$$

where  $P(qLM_L)$  is the probability of finding an atomic pair in an internal state  $|qLM_L\rangle$  due to thermal distribution. We assume that the system is in thermal equilibrium with temperature  $T > T_{BEC}$  higher than the condensation temperature. The partition function of a pair confined in a sphere of radius  $R$  is given by [19]

$$\mathcal{Z} = \sum_{n \in \text{bound states}} e^{-\beta E_n} + \frac{1}{\pi} \int_0^\infty dq \sum_{L=0}^{L_{max}} (2L+1) \left( R + \frac{d\delta_L}{dq} \right) e^{-\beta \hbar^2 q^2/m}. \quad (13)$$

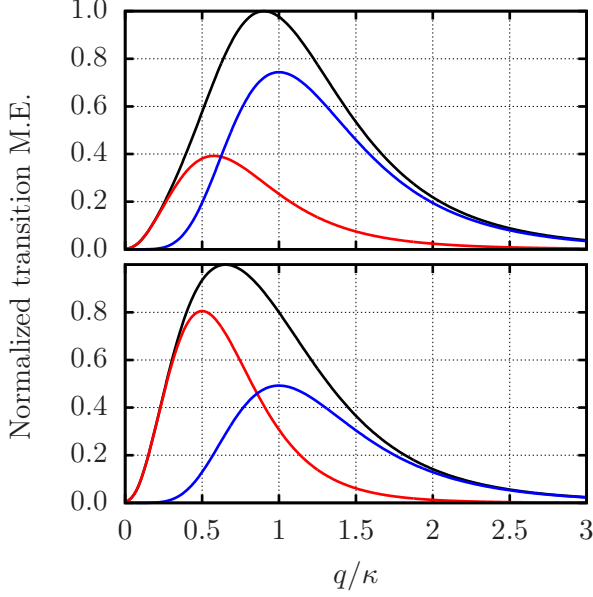


FIG. 1. (Color online) The normalized 2-body transition matrix element, Eq. (8), as a function of the relative momentum  $q/\kappa$ . The sum (black), the  $r^2$  (red, peaked at  $q = \kappa/2$ ) and quadrupole (blue, peaked at  $q = \kappa$ ) terms are given for  $a/r_{eff} = 2$  (upper panel) and  $a/r_{eff} = 200$  (lower panel).

Given  $q$ , finite  $R$  imposes a cutoff  $L_{max} \approx qR$  on  $L$ . For  $L = 0, 2$  and large enough  $R$  we can safely assume that  $P(qLM_L) = P(q) = \frac{1}{2} \frac{R}{\pi} e^{-\beta \hbar^2 q^2/m}$ .

The sum  $\sum_f$  contains all possible dimer quantum numbers and all possible photons weighted by the emission function,

$$\sum_f = \frac{\Omega}{(2\pi)^3} \sum_{\rho, L', M'_L} \int d\mathbf{k} (1 + N_{\mathbf{k}\rho}), \quad (14)$$

where  $N_{\mathbf{k}\rho}$  is the number of photons with momentum  $\mathbf{k}$  and polarization  $\rho$  in the initial state. The stimulating rf radiation is a narrow distribution centered at some  $\mathbf{k}_{rf}$ . Therefore  $N_{\mathbf{k}\rho} \approx N_{\mathbf{k}_{rf}\rho_{rf}} \delta(\mathbf{k} - \mathbf{k}_{rf}) \delta_{\rho, \rho_{rf}} / \Omega$ , where  $\mathbf{k}_{rf}$  is the momentum of the stimulating rf field and  $\rho_{rf}$  is its polarization.

Substituting Eqs. (8), (12), (14) into Fermi's golden rule (2), the dimer formation rate is given by

$$r_{i \rightarrow f} = \frac{g^2 \mu_B^2 c k_{rf}^5 m N_{\mathbf{k}_{rf}\rho_{rf}} P(q)}{16(2\pi)^2 \hbar^2 q \Omega} |\langle S_0 \rangle|^2 \sin^2 \gamma \sin^2 \beta \left( \frac{1}{6^2} I_s^2 + \frac{5}{15^2} I_d^2 \right). \quad (15)$$

The relative momentum  $q$  is connected to the photon wave number through energy conservation  $\hbar^2 q^2/m = E_B + \hbar c k_{rf}$ .

The relative importance of  $s, d$  modes shifts with temperature. This point is demonstrated in Figs. 2 and 3. In Fig. 2 we present the  $s, d$  rates to the photoassociation

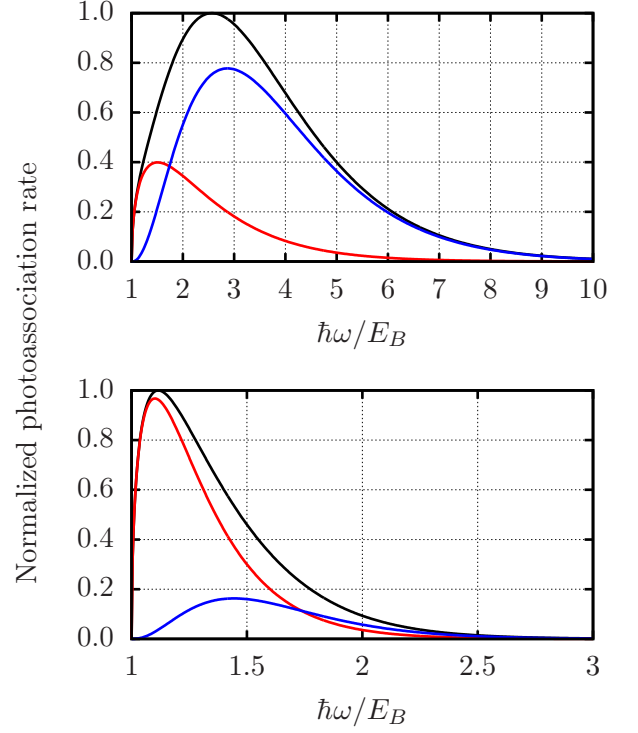


FIG. 2. (Color online) Normalized dimer photoassociation rate as a function of rf photon frequency. The total (black), the  $r^2$  (red, low energy peak) and the quadrupole (blue) rates are presented for  ${}^7\text{Li}$  with  $a_s = 1000a_0$  at  $T = 5\mu\text{K}$  (lower panel) and at  $T = 25\mu\text{K}$  (upper panel).

of  ${}^7\text{Li}$  dimers at  $a = 1000a_0$ ,  $a_0$  is the Bohr radius, for  $T = 5\mu\text{K}$  and  $T = 25\mu\text{K}$ . The relative contribution of the  $r^2$  and quadrupole to the resonance peak is displayed in Fig. 3. It is evident that at low temperatures the  $s$  mode is dominant. The importance of the  $d$  mode grows with the ratio  $k_B T/E_B$ . Therefore we can conclude that for small  $k_B T/E_B$  values the photoassociation is an  $s$ -wave process while for large values it is a  $d$ -wave process.

Summing up, in this work we have studied the photo response of ultra-cold atomic gases. Comparing spin-flip and frozen-spin experiments we have found that the reaction mechanism is quite different in these two processes. While the spin-flip reaction is dominated by the well known Frank-Condon factor, for frozen-spin process the reaction rate is governed by the two competing  $r^2$  and quadrupole modes. Comparing the relative strength of these modes in dimer photoassociation we predict that the mutual importance of these two modes changes with temperature and scattering length. The implications of these results on photoassociation experiments and on trimer formation rates is yet to be studied.

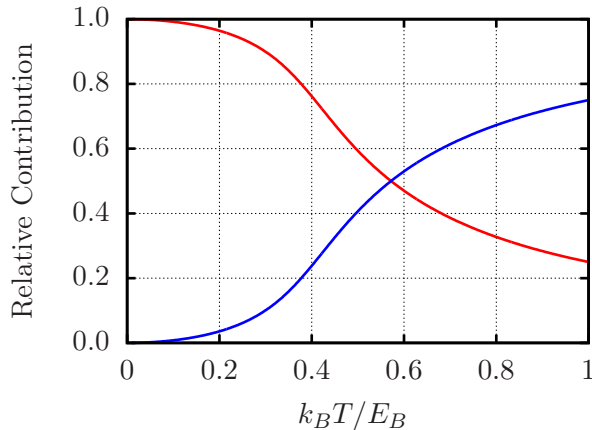


FIG. 3. (Color online) The relative contribution of the  $s$  (red, light grey) and  $d$  modes to the resonance peak as a function of temperature  $k_B T / E_B$ .

## ACKNOWLEDGEMENTS

This work was supported by the ISRAEL SCIENCE FOUNDATION (Grant No. 954/09). The authors would like to thank L. Khaykovich, S. Jochim, and N. Nevo Dinur for their useful comments and suggestions during the preparation of this work.

- 
- [1] C. Greene, *Physics Today*, **40** (March 2010).
  - [2] E. Braaten and H.-W. Hammer, *Phys. Rep.* **428**, 259 (2006).
  - [3] S. T. Thompson, E. Hodby, and C. E. Wieman, *Phys. Rev. Lett.* **95**, 190404 (2005).
  - [4] S. B. Papp and C. E. Wieman, *Phys. Rev. Lett.* **97**, 180404 (2006).
  - [5] C. Weber, G. Barontini, J. Catani, G. Thalhammer, M. Inguscio, and F. Minardi, *Phys. Rev. A* **78**, 061601R (2008).
  - [6] T. Lompe et al., *Science* **330**, 940 (2010).
  - [7] N. Gross, Z. Shotan, S. Kokkelmans, and L. Khaykovich, *Phys. Rev. Lett.* **105**, 103203 (2010).
  - [8] N. Gross, Z. Shotan, O. Machtey, S. Kokkelmans, and L. Khaykovich, *C. R. Physique* **12**, 4 (2011).
  - [9] S. Nakajima, M. Horikoshi, T. Mukaiyama, P. Naidon, and M. Ueda, *Phys. Rev. Lett.* **106**, 143201 (2011).
  - [10] O. Machtey, Z. Shotan, N. Gross and L. Khaykovich, *Phys. Rev. Lett.* **108**, 210406 (2012).
  - [11] C. Chin, and P. S. Julienne, *Phys. Rev. A* **71**, 012713 (2005).
  - [12] J. F. Bertelsen and K. Molmer, *Phys. Rev. A* **73**, 013811 (2006).
  - [13] Th. M. Hanna, Th. Kohler, and K. Burnett, *Phys. Rev. A* **75**, 013606 (2007).
  - [14] C. Klempt, T. Henninger, O. Topic, M. Scherer, L. Kattner, E. Tiemann, W. Ertmer, and J. J. Arlt, *Phys. Rev. A* **78**, 061602R (2008).
  - [15] E. Liverts, B. Bazak, and N. Barnea, *Phys. Rev. Lett.* **108**, 112501 (2012); B. Bazak, E. Liverts, and N. Barnea, *Few-body sys. accepted for publication* (2012).
  - [16] We adopt the Heaviside-Lorentz units in this paper.
  - [17] B. R. Levy and J. B. Keller, *J. Math. Phys.* **4**, 54 (1963).
  - [18] L. D. Landau, E. M. Lifshitz, *Quantum Mechanics* 3rd Ed., (Pergamon Press, New York, 1991).
  - [19] L. D. Landau, E. M. Lifshitz, *Statistical Physics* 3rd Ed., (Pergamon Press, New York, 1980).